Macroscopic observations of diel fish movements around a shallow water artificial reef using a mid-frequency horizontal-looking sonar

Wu-Jung Lee[a)] and Dajun Tang
Applied Physics Laboratory, University of Washington, 1013 Northeast 40th Street, Seattle, Washington 98105, USA

Timothy K. Stanton
Department of Applied Ocean Physics and Engineering, Woods Hole Oceanographic Institution, 86 Water Street, Woods Hole, Massachusetts 02543, USA

Eric I. Thorsos
Applied Physics Laboratory, University of Washington, 1013 Northeast 40th Street, Seattle, Washington 98105, USA

The twilight feeding migration of fish around a shallow water artificial reef (a shipwreck) was observed by a horizontal-looking, mid-frequency sonar. The sonar operated at frequencies between 1.8 and 3.6 kHz and consisted of a co-located source and horizontal line array deployed at 4 km from the reef. The experiment was conducted in a well-mixed shallow water waveguide which is conducive to characterizing fish aggregations at these distances. Large aggregations of fish were repeatedly seen to emerge rapidly from the shipwreck at dusk, disperse into the surrounding area during the night, and quickly converge back to the shipwreck at dawn. This is a rare, macroscopic observation of an ecologically-important reef fish behavior, delivered at the level of aggregations, instead of individual fish tracks that have been documented previously. The significance of this observation on sonar performance associated with target detection in the presence of fish clutter is discussed based on analyses of echo intensity and statistics. Building on previous studies of long-range fish echoes, this study further substantiates the unique utility of such sonar systems as an ecosystem monitoring tool, and illustrates the importance of considering the impact of the presence of fish on sonar applications. © 2018 Acoustical Society of America.
https://doi.org/10.1121/1.5054013

[JAC]   Pages: 1424–1434

I. INTRODUCTION

Vertical-looking, high-frequency echosounders are widely used in fisheries and marine ecological studies to "image" organism distributions in the water column (Stanton, 2012; Benoit-Bird and Lawson, 2016). However, the narrow horizontal coverage of these systems makes them largely incompatible with observing horizontal spatial distributions of organisms that are capable of moving rapidly, such as fish. Horizontal-looking sonar systems provide a promising avenue to address this issue by delivering real-time data that encompass a spatial area from a few kilometers to tens of kilometers (Urick, 1983). At low to mid frequency ($\lesssim$10 kHz), sonar broadcasts can elicit strong echoes from fish whose swimbladders resonate and scatter sound strongly in this band (Medwin and Clay, 1998), making it possible to observe fish aggregation and movement over long ranges. Such capability was first demonstrated in a series of experiments in the late 1960s (e.g., Rusby *et al.*, 1973; Weston and Andrews, 1990; Weston and Revie, 1971), and more recently to image highly dynamic pelagic

fish shoals over the scale of a continental shelf (e.g., Gauss *et al.*, 2009; Jones *et al.*, 2017; Makris *et al.*, 2006; Makris *et al.*, 2009). In these studies, strong diel changes of fish behavior were reported, with varying spatiotemporal patterns depending on the seasonal and ecological context.

An important insight from the above studies is that the interaction of sound with ocean boundaries (sea surface and seafloor) and water column sound speed variabilities can make biological interpretation of echoes from a horizontal-looking sonar a challenging task (Gauss *et al.*, 2004; Jones *et al.*, 2014; Jones *et al.*, 2017; Pedersen and Trevorrow, 1999). For example, the presence of convergence and shadow zones in the waveguide can cause dramatic changes in the echo returns from fish as they move across different zones in the water column. This can result in significant ambiguity in the interpretation (see Fig. 5 in Jones *et al.*, 2014 for an illustration).

In this study, we analyze data from the Target and Reverberation Experiment 2013 (TREX13, see Hefner and Tang, 2017a,b; Yang *et al.*, 2018), which provided a unique data set for isolating and understanding the long-range scattering contribution from fish in shallow-water coastal environments. The experiment was designed to understand the

physical mechanisms that contribute to sound scattering and reverberation underwater and was performed in a well-mixed ocean waveguide that was in general evenly ensonified (Tollefsen and Pecknold, 2014). The fish echoes were collected by a mid-frequency, horizontal-looking sonar system, and the sound propagation condition and fish behavior differ significantly from the pelagic and riverine environments that were studied previously. Specifically, the experimental environments in previous studies were much more complex in terms of bathymetry and sound speed profile, which limited the interpretation of echoes from fish as discussed above. In TREX13, the very shallow (∼20 m depth; Fig. 1), nearly flat seafloor and the well-mixed water column formed a relatively simple waveguide, which is more conducive to interpretation of fish echoes (Tollefsen and Pecknold, 2014). In addition, the fixed source and fixed receiver array (both bottom mounted) ruled out variability caused by movement of measurement systems, which further simplified the interpretation of the temporal evolution of the sonar data.

Strong fish echoes were seen to dominate the echo returns at night throughout the 20-day span of data collection (Yang et al., 2018), making observation of "clean" reverberation signals from solely physical sources, such as waveguide boundaries—the primary goal of investigation of TREX13—difficult during a significant portion of the experiment. Here we focus our analysis on the rapidly changing echo patterns from fish as they diverged from and converged back to a known artificial reef for nocturnal foraging (Fig. 2). The artificial reef was a shipwreck that functions as daytime shelter for the fish (Appeldoorn et al., 2009). During dusk and dawn, the fish's movements encompassed an area of several kilometers within a short time period (∼30 min). Such a macroscopic observation of the twilight foraging migration of reef fish is to our knowledge not available in the literature, as all previous accounts were based on diver- or camera-based survey, or tagging of individual fish (e.g., Appeldoorn et al., 2009; Myers et al., 2016; Nagelkerken et al., 2000). Our sonar study thus has implications in resource management in view of the controversy over artificial reef as a habitat restoration tool (Bohnsack, 1989; Pickering and Whitmarsh, 1997).

The predictable emergence, dispersal, and re-congregation of reef fish in association with the shipwreck in TREX13 also provides an outstanding opportunity for investigating the influence of fish echoes on sonar target detection. Specifically, the variable forms of fish aggregations can produce strong echoes that are similar to those from geological features (i.e., reverberation), which could mask the target signals, as well as echoes that are akin to those from human-made objects, which could trigger false alarms (i.e., clutter; Gauss et al., 2009; Gelb et al., 2010; Jones et al., 2014). Both classes of effects were observed in our study as the reef fish aggregation morphed into different spatial patterns around the shipwreck. By detailing the data collection and analysis, our primary goal of the paper is to investigate the influence of fish echoes on sonar detection applications. We also strive to point out the unique potential of using similar sonar methods to study fish behavior in reef environments.
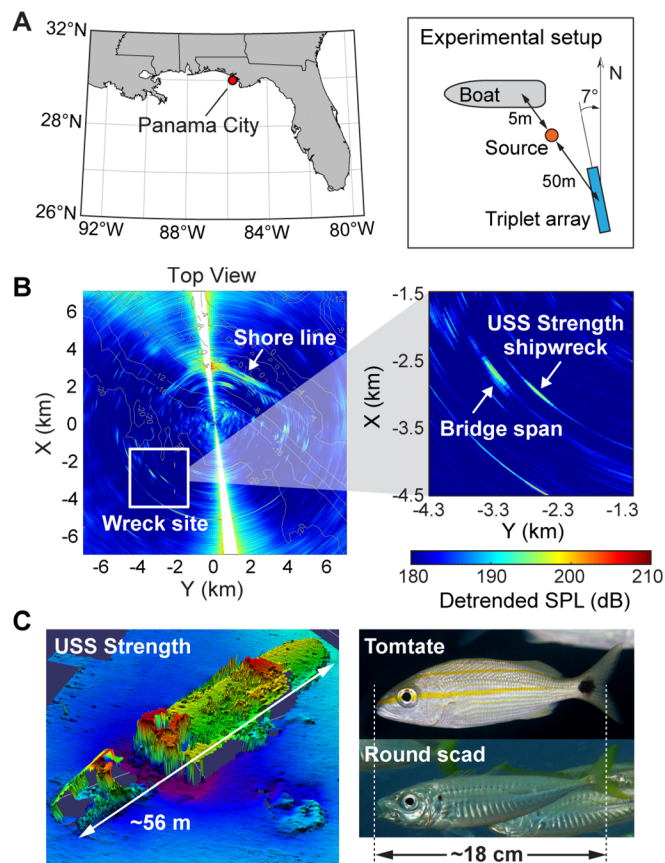

FIG. 1. (Color online) Overview of experiment. (A) Location of the TREX13 experiment and the reverberation experimental setup (drawing not to scale). (B) An example echogram (bird's-eye view) obtained from cardioid beamforming and pulse compression, with bathymetry overlaid. Analyses in this study are focused in the rectangular area that includes the shipwreck of USS Strength. SPL: Sound Pressure Level. (C) A multibeam reconstruction of the shipwreck of USS Strength (Orange and Garcia-Garcia, 2010) and images of the two dominant fish species in the area. Fish pictures are from FishBase, http://www.fishbase.org/.

II. OVERVIEW OF EXPERIMENT

A. Acoustic data collection

The TREX 13 experiment was conducted approximately 2 km offshore near Panama City Beach, FL, where the water depth is approximately 20 m [Fig. 1(A)]. During the experiment, sonar signals were transmitted from a fixed, horizontally omnidirectional source (ITC-2015), and the echo returns were recorded by a nearby fixed triplet hydrophone array (FORA, Haralabus and Baldacci, 2006). Different from regular linear arrays, a triplet array consists of a line of hydrophone triplets made of three closely-spaced omnidirectional hydrophones, forming an equilateral triangle, with the plane of the triplet being perpendicular to the physical array axis. The array used in the experiment contained 48 triplets (a total of 144 elements) equally spaced at 0.2 m, resulting in a total array length of 9.4 m. The triplet design allowed cardioid beamforming, which helped resolving the left-right ambiguity in regular linear arrays (see Sec. III A for detail). The radius of each triplet was 0.0222 m. The array was deployed horizontally in the water column and oriented such that the bearing at the end-fire direction was 7° from true north [Fig. 1(A)].

J. Acoust. Soc. Am. **144** (3), September 2018
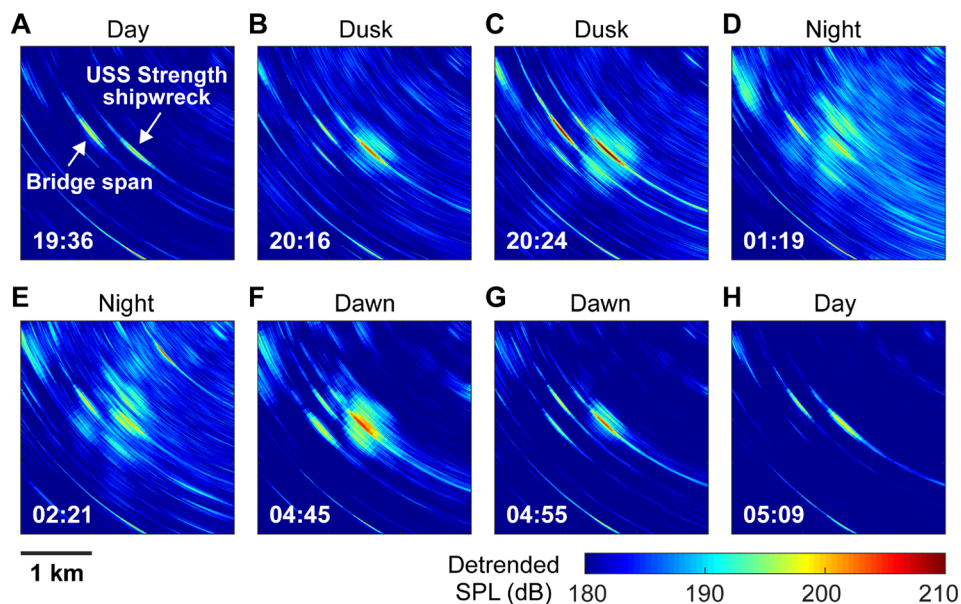
Lee *et al.* 1425

FIG. 2. (Color online) A series of echograms showing fish movement over time. Fish were observed to emerge from the shipwreck at dusk (A), (B), disperse into the surrounding area during the night (C)–(E), and converge back to the shipwreck at dawn (F), (G). Each echogram was obtained from a single sonar ping. A range-varying gain of $30 \log_{10} R$ (where R is the range in meters) was added to the echograms to compensate for the approximate transmission loss over range. All echograms shown in this study except for Fig. 6 were detrended following this convention. Panel (A) is identical with Fig. 1(B). Local time (24 h clock) is given in the lower left corner of each panel. Data shown are from experimental session #131 conducted on May 16, 2013.

The sonar data analyzed in this study were from six overnight experimental sessions during May 9–16, 2013 (Table I). The sessions started in the evenings and ended approximately two hours after dawn. A variety of linear frequency-modulated (LFM) signals with different bandwidths within the range of 1.8–3.6 kHz were broadcast at different source levels near 200 dB before pulse compression (Table I). The received echoes were pre-amplified and sampled at 12.5 kHz. We focused our analysis in an area surrounding the shipwreck of USS Strength in the southwest quadrant of the sonar observation range [Fig. 1(B)].

B. Physical environment for sound propagation

The acoustic experiment was accompanied by an extensive suite of sampling of the physical environment that was designed to reduce ambiguities in echo interpretation. The environmental sampling ranged from the sea surface, water column, seafloor and sediment, and included measurements such as sound speed profile, multi-beam bathymetry mapping, sediment properties, surface wind, wave height, and wave direction (see Hefner and Tang, 2017a,b for an overview). The combination of the well-mixed water column, the nearly flat bottom, and the moderate bandwidth of the transmit signals jointly resulted in approximately even ensonification of scatterers irrespective of depth. The interpretation of fish echoes is thus more straightforward due to the absence of prominent shadow zones or convergence zones in the waveguide.

C. Dominant fish species

The sunken shipwrecks and bridge sections function as artificial reefs in the local ecosystem, and are popular recreational diving sites owing to the enormous abundance of reef fish (Stolk et al., 2007). While no direct biological sampling was conducted during TREX13, potentially dominant fish species were identified based on visual observation during the experiment (by T.K.S.). Multiple sources of references were used to corroborate this observation, including a video-based survey (Patterson et al., 2013), a video taken at the USS Strength shipwreck about a month after TREX13 (Nieto, 2013), and amateur diver's records compiled by Reef Environmental Education Foundation at the location USS Strength (Panama City) (REEF, https://www.reef.org/db/reports/geo, Region: Tropical Western Atlantic, Zone Code: 21010007). The most likely dominant fish species included tomtate (*Haemulon aurolineatum*) and round scad (*Decapterus punctatus*) [Fig. 1(C)]. Both species and their associated taxa have been widely reported to be particularly abundant in artificial reef environments (Arena et al., 2007; Patterson et al., 2013). Given the nominal water depth at the experimental site (20 m), the size of the fish (and its swimbladder) and the fact that both species are physoclists whose swimbladder volume remains constant irrespective of depth, the sonar frequencies employed in TREX13 are likely near or slightly above the swimbladder resonance of these species (see Fig. 3 in Stanton et al., 2012) and can yield strong echo responses.

III. ACOUSTIC DATA ANALYSIS

A. Beamforming and pulse compression

Beamforming and pulse compression were applied to the receiver array recordings to extract spatial information from echoes. Taking advantage of the triplet arrangement of array elements, cardioid beamforming (Haralabus and Baldacci, 2006) was performed to disambiguate echoes originating from the starboard and port side of the array. The beamforming processing was conducted coherently in the frequency domain without averaging over the signal bandwidth in order to preserve the phase information for echo statistics analysis. This is different from the processing employed in Yang et al. (2018), where the beamformed complex echo returns were incoherently combined over the signal bandwidth. The frequency-dependent cardioid calibration factor [Eq. (23) in Haralabus and Baldacci, 2006] was used due to the broad signal bandwidths. The array geometry resulted in an azimuthal beamwidth of 2.2°. However, the

TABLE I. The date, time of observation, and signals used during the overnight sessions of the TREX experiment. Detailed analyses were conducted using data from experimental session #131 because the sonar time series was the longest among all sessions with the widest signal bandwidths.

Session number	Date[a]	Time of observation (local time)	Frequency coverage of transmit signals[b] (kHz)	Number of waveforms	Maximum waveform bandwidth	Source level (dB)
79	May 9	21:29–07:15	1.8–3.6, 6.6–8.4	9	NB[c] to 1800 Hz	195–198.3[d]
87	May 10	17:52–07:00	3.5–3.6	1	100 Hz	198.3
94	May 11	20:15–07:15	1.8–3.5	3	200 Hz	195.5, 196.8, 198.2
115	May 13	20:51–07:00	1.8–3.6	2	900 Hz	196.7, 195
124	May 15	21:13–08:19	1.8–3.6	2	900 Hz	196.7, 195
131	May 16	19:00–07:29	1.8–3.6	2	900 Hz	196.7, 195

[a]Date overnight session began.
[b]The frequencies shown here are the bandwidth covered by different transmit waveforms. The bandwidth of each individual waveform ranged from 100 to 1800 Hz.
[c]Narrowband (NB) waveforms were gated sinusoidal waves.
[d]The 6.6–8.4 kHz waveform was transmitted with source level at 187.1 dB, because this frequency range was outside of the most efficient band of the transducer.

beamforming operation was performed at $1°$ increments to (1) obtain smoothed sonar images, and (2) facilitate the estimation of the probability distribution of echo amplitude. To improve the sonar range resolution, pulse compression was subsequently performed on the beamformed echo data by using the transmit signal as the replica. As an example, the nominal range resolution achieved by pulse compression was approximately 0.83 m for the 900-Hz bandwidth LFM signals used in experimental session #131. The final processed echo returns were plotted as a function of beam angle and range [the "echogram," Fig. 1(B)] assuming a nominal sound speed of 1525 m/s (Tollefsen and Pecknold, 2014). For all echograms presented in this study, a range-varying gain of $30 \log_{10} R$ (where R is the range in meters) was added to the echo time series (except for Fig. 6) to compensate for the approximate transmission loss over range.

B. Selection of analysis windows

Three analysis windows on the echogram were selected to quantify changes of the fish and shipwreck echoes over time [Figs. 3(A) and 4(A)]. Analysis window 1 (AW1) was chosen to enclose the shipwreck of USS Strength and the immediately adjacent area. This window encompasses an angular range of $10.89°$ and spans a range between 3.92 and 4.12 km, which includes a total of 39 360 digitized echo samples. Analysis window 2 (AW2) was chosen to enclose an area right next to AW1, toward which the fish dispersed into after dusk. It encompasses an angular range of $10.89°$ and spans a range between 3.72 to 3.92 km, and includes the same number of samples as AW1. Analysis window 3 (AW3) is irregular in shape and was chosen in an ad-hoc manner to enclose both the shipwreck and a large portion of the emerged fish during the night but exclude the strong echoes from the nearby sunken bridge section. Note that each analysis window includes "cross-angle" samples from a single ping, as oppose to "cross-ping" samples from only one beam.

C. Summary statistics of echo returns

Three summary statistics were calculated for the echoes in sample windows AW1 and AW2: (1) the probability distribution

of the echo envelope [the "echo probability density function" (echo pdf)], (2) the maximum echo level (E_{max}), and (3) the scintillation index (SI). All statistics were obtained using the beamformed, pulse-compressed echo samples without the range-varying gain that was applied to the echogram. Since the analysis windows were within a narrow range span, whether or not the gain was applied would not result in significant differences.

The echo pdf is the distribution of instantaneous samples of echo magnitude (i.e., envelope). This is a "first-order" statistic that summarizes the composition of echo samples across the full range of echo magnitude fluctuations within the analysis window. The echo pdf characterizes the probability of an echo magnitude originating from target(s) of interest, and can be obtained either empirically or theoretically depending on the context (e.g., Chu and Stanton, 2010; Fialkowski and Gauss, 2010). Here, the echo pdf was estimated using the kernel density method (KDE, Botev et al., 2010) based on the ensemble of all echo samples enclosed in the analysis window. The shape of the echo pdf is closely related to the physical scattering processes (Chu and Stanton, 2010; Stanton et al., 2018). In the case in which the echoes are from a large number of similar scatterers producing significantly overlapping echoes, both the real and imaginary components of the echoes would tend toward the Gaussian distribution (with a zero mean), making the resultant echo pdf Rayleigh-like. In other cases, the non-Rayleigh shape of the echo pdf may provide information for interpreting the sources of scattering, such as the group composition and the number of scatterers ensonified by the sonar (Lee and Stanton, 2014, 2016; Stanton et al., 2015).

E_{max} is the maximum value of all echo samples enclosed within an analysis window. It is an "extremal" statistic, since this quantity represents the maximum value across many independent random variables. E_{max} is a function of both the first-order statistics of the instantaneous value of the echo (i.e., the "echo pdf" above) and the number of independent samples (or, equivalently, size of analysis window). Generally, the larger the number of independent samples (or analysis window), the more biased the peak sample will be toward higher amplitudes. Echo peak statistics within a window is useful in studying the tail of a distribution which

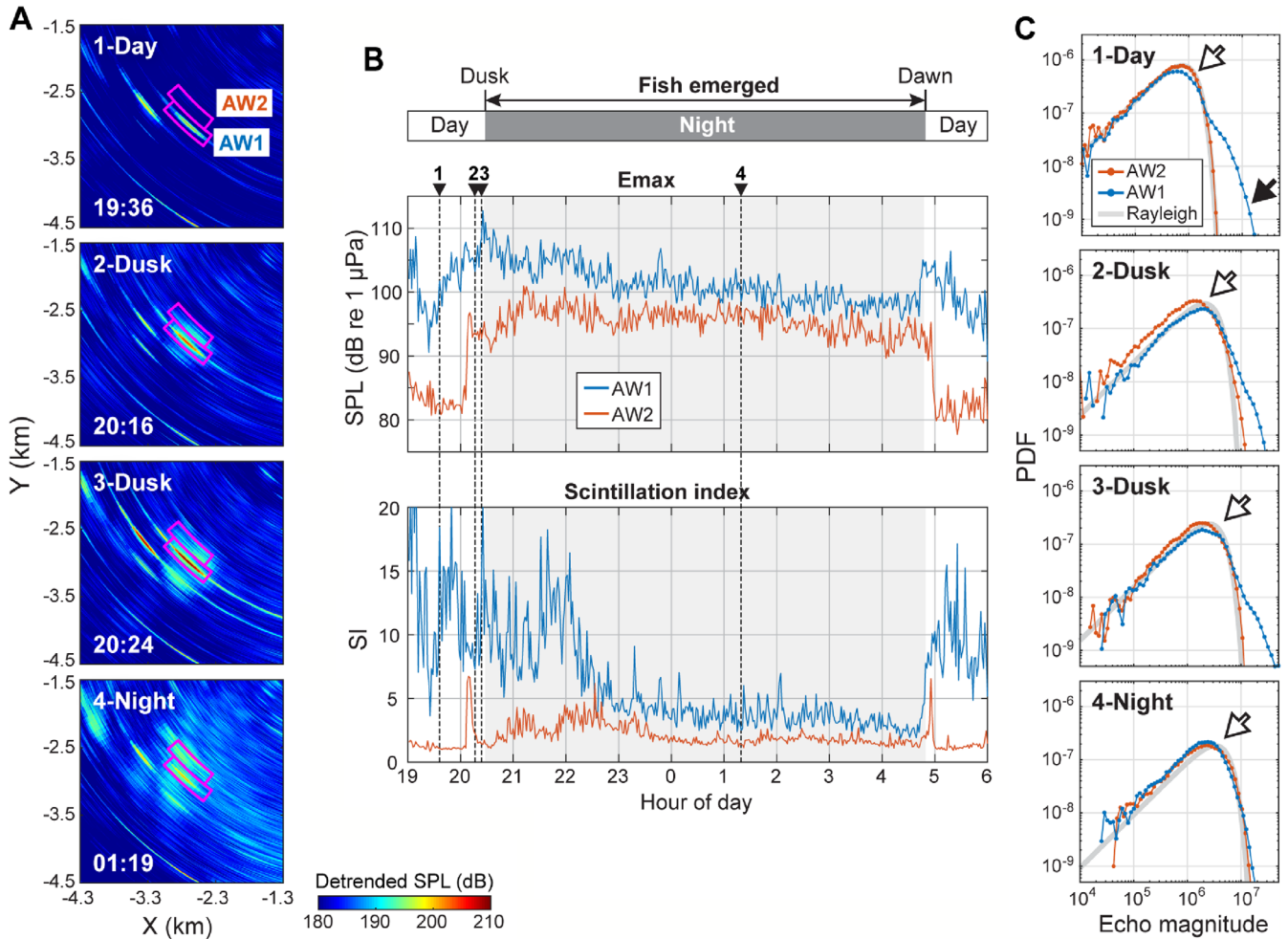J. Acoust. Soc. Am. **144** (3), September 2018

Lee et al. 1427

FIG. 3. (Color online) Variation of echo level and associated statistics during experimental session #131 on May 16, 2013 (Table I). (A) A series of echograms showing fish movement in relation to the two analysis windows, based on which detailed analyses were conducted. Analysis window 1 (AW1) encloses the region immediately adjacent to and including the shipwreck of USS Strength. Analysis window 2 (AW2) encloses a nearby region the emerged fish expanded into during the night. (B) Time series of maximum echo level (top) and scintillation index (bottom) of the echoes enclosed by AW1 and AW2. The sonar transmission times for the echograms in (A) are plotted as vertical dashed lines for reference. (C) Probability density function of the envelope amplitudes of echoes in AW1 and AW2 for the pings shown in (A). The scale parameter of the Rayleigh distribution was estimated based on the mean echo energy in AW2 (see text). Note that the tail of the echo pdf in AW1 (black arrow in panel 1) continued to increase at dusk as fish emerged from the shipwreck. The echo pdfs of both AW1 and AW2 are both Rayleigh-like during the night (panel 4). The variations shown here were reversed at dawn when fish converged back to the shipwreck (see Fig. 2). All pdfs are plotted using the same arbitrary horizontal scale ("echo magnitude").

contains information about the largest scatterer within the window (Stanton, 1985).

The *SI* quantifies the deviation of echo pdf from the Rayleigh distribution through $SI = \langle (A^2/\rho c - \lambda_R)^2 \rangle / \lambda_R^2$, where A is echo amplitude and λ_R is the mean echo intensity of the echo ensemble (Gallaudet and de Moustier, 2003). *SI* is equivalent to the variance of echo intensity normalized by the square of mean intensity. For Rayleigh-distributed echoes, $SI = 1$.

In addition to the above summary statistics, the total echo energy E_T from AW3 was also computed to gain a global understanding of the overall echo variation throughout the course of fish movements during the night. E_T was calculated by incoherent summation (in the linear domain) of all echo samples enclosed in AW3.

D. Split-window echo normalizer

The split-window mean-amplitude normalizer is a data-driven method commonly used in sonar detection

applications to detrend echo data and extract regions containing potential targets of interest (Abraham and Willett, 2002; Fialkowski and Gauss, 2010). The normalizer is designed to improve detection performance by mitigating the effects of mean echo decay as a function of range in the waveguide or locally elevated reverberation from extended non-target echo sources, such as ridges, sand waves, or other geographical features. The normalization is accomplished by running a sliding window along range and normalizing the power of the cell at the center of the sliding window by the mean power of local reverberation and background noise within the window. The sliding window consists of a pair of "guard bands" and a pair of "auxiliary bands." The guard bands are immediately adjacent to the center cell to be normalized, and are excluded from the estimation of mean reverberation and noise power in order to reduce the influence of pulse compression sidelobes (see Fig. 2 in Abraham and Willett, 2002). The auxiliary bands are samples within the sliding windows but outside of the guard bands. In this

study, the width of each guard band was chosen to be twice the inverse of bandwidth (2/bandwidth). The width of each auxiliary band was chosen to be equivalent to a 200 m range bin. This parameter combination is identical to those used in Jones *et al.* (2017).

IV. BIOLOGICAL INTERPRETATION OF SONAR ECHOES

The dramatic fish movements shown in Fig. 2 were repeatedly observed in all overnight experimental sessions (see Sec. IV B for quantification). In this paper, only results from experimental session #131 (May 16, 2013) are discussed in detail to avoid redundancy. Session #131 was chosen because this sonar time series was the longest (from May 16, 19:00 to May 17, 07:29) with the widest signal bandwidths (two waveforms with 900 Hz bandwidths: 1.8–2.7 kHz and 2.7–3.6 kHz, with source levels at 196.7 dB and 195.0 dB, respectively; see Table I). Below we discuss the changing patterns of echo returns from a biological perspective.

A. Sonar observation of twilight fish migration

Significant variation in the strength and distribution pattern of echo returns was observed near the USS Strength shipwreck in all overnight experimental sessions investigated in this study. Every day, large aggregations of fish were observed to emerge from the shipwreck at dusk, disperse into the surrounding areas during the night, and converge back to the shipwreck right before dawn (Fig. 2, Mm. 1, Mm. 2). Before dusk, strong echoes were only seen at the shipwreck locations [Fig. 2(A)]. As the ambient light level dimmed [Figs. 2(B) and 2(C)], the high-echo-energy patch started to spread from the USS Strength shipwreck location, and eventually morphed into a more diffused pattern past midnight [Figs. 2(D) and 2(E)]. Before dawn, the dispersed echo pattern in the night converged again rapidly until the strong shipwreck echo signature reappeared [Figs. 2(F)–2(H)]. These movements were observed across an area of approximately 4 km². The expansion and shrinking speed at the edges of the high-echo-energy patch was estimated to be approximately 0.2–0.4 m/s. This is similar to the typical speed at which reef fish swim (Fulton *et al.*, 2005). The rapid changes in sonar echo patterns were attributed to fish scattering due to (1) the proximity of the sonar frequency to the swimbladder resonance of dominant fish species in the area, (2) the rapid, spatially- and temporally-coupled variation of the distribution of strong echo returns, and (3) the fact that the shipwrecks are highly productive artificial reefs (Bohnsack, 1989; Patterson *et al.*, 2013).

Mm. 1. A video of consecutive echograms showing fish emergence from the shipwreck at dusk. This is a file of type "mp4" (5.3 Mb).

Mm. 2. A video of consecutive echograms showing fish convergence back to the shipwreck at dawn. This is a file of type "mp4" (4.5 Mb).

The macroscopic diel horizontal movements of reef-associated fish shown in this study is a biological phenomenon that to our knowledge has not been observed before using horizontal-looking sonar systems. For reasons given in the previous paragraph, it is likely that the actual dusk dispersal and dawn re-aggregation of reef fish were directly captured in the sonar echo return. This is different from the rapid formation and disbandment of pelagic fish shoals reported previously (e.g., Weston and Revie, 1971; Makris *et al.*, 2009). There, the variations of echo patterns were primarily driven by the convergence of scattered fish already residing in the same area. Fish echoes only became observable when the numerical density of fish (number per unit area) is above a minimum detectable density determined by the reverberation environment (Farmer *et al.*, 1999; Makris *et al.*, 2006). Therefore, the appearance of shoals in the echogram was at a speed much faster than that of individual fish in these former studies.

B. Timing and spatial pattern of fish movements

The timing of fish movements can be quantified by examining the variation of E_{max} in AW1 and AW2 [$E_{max,\,AW1}$ and $E_{max,\,AW2}$, respectively; Figs. 3(A) and 3(B)]. $E_{max,\,AW1}$ is equivalent to the *apparent* echo level of the shipwreck of USS Strength, since echoes originating from the shipwreck location were always the strongest within AW1. It is the *apparent*, not necessarily the actual, echo of the shipwreck because the shipwreck echo may have contained contributions from collocated fish (see Sec. IV C for detailed discussion). $E_{max,\,AW2}$ is the strongest echo from either a water column that was likely empty (note the low backscattering level) before dusk or the fish aggregation dispersing into AW2 during the night.

The ping-by-ping E_{max} time series show a tight correlation of fish movement with the ambient light cycle [Fig. 3(B)]. Specifically, $E_{max,\,AW1}$ increased initially as fish emerged out of the shipwreck before dusk (1930–2030) and started to decrease gradually at dusk (~2030) until abruptly raising back right before dawn (~0450). $E_{max,\,AW2}$ increased sharply as fish dispersed out from the shipwreck around dusk (2000–2030) and dropped equally rapidly as fish converged back to the shipwreck around dawn (~0500). Using $E_{max,\,AW2}$ as an indicator of the spatial extent of fish movement, we found that the dispersal and congregation of reef fish were reliably repeated in synchrony with the light cycle for all overnight experimental sessions (Fig. 5).

The total echo energy E_T enclosed in AW3 provides a similar metric to capture not only the timing, but also the spatial extent of fish movements (Fig. 4). Specifically, E_T was not conserved throughout the course of fish movements. E_T increased sharply as fish emerged from the shipwreck at dusk [Fig. 4(B); 1930–2030]. This change was reversed as fish converged back to the shipwrecks at dawn [Fig. 4(B); ~0500]. In addition, E_T slowly decreased after midnight as more fish visibly moved out of AW3 on the echogram [e.g., comparing panel 2 and 3 in Fig. 4(A)]. Importantly, the rapid change of E_T closely tracks the change of $E_{max,\,AW1}$, which was tightly correlated with $E_{max,\,AW2}$ and the light cycle [Fig. 3(B)].

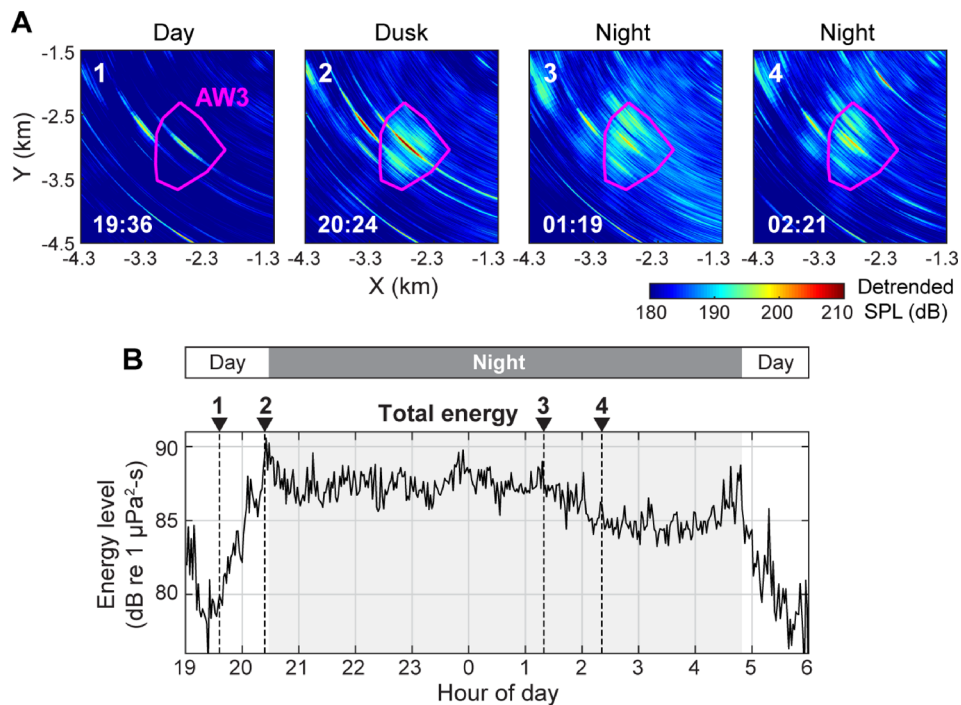J. Acoust. Soc. Am. **144** (3), September 2018

Lee *et al.*   1429

FIG. 4. (Color online) Correlated variation of echo energy and fish movement. (A) Example echograms showing fish movement with respect to the shipwreck and an irregularly-shaped analysis window AW3. AW3 was selected to enclose a large portion of the emerged fish during the night and includes the shipwreck. (B) Time series of total echo energy in AW3. The total echo energy increases as fish started to emerge from the shipwreck, decreased gradually after 1 AM as more fish moved out of AW3, increased again right before dawn as fish moved toward the shipwreck, and decreased again when fish converged back to the shipwreck. The sonar transmission times for the echograms shown in (A) are plotted as vertical dashed lines in (B).

Similar E_T variation was observed in other experimental sessions, in particular during the dawn period where more data are available. The detailed E_T variation between dusk and dawn varied from night to night due to differences in fish dispersal pattern with respect to the boundary of AW3.

C. Detailed fish aggregation pattern

Changes in the echo pdfs from AW1 and AW2 (PDF$_{AW1}$ and PDF$_{AW2}$, respectively) were tightly linked to the emergence, dispersion, and re-aggregation of fish throughout the night. The echo pdf changes also coincided with variations in SI, E_{max}, and E_T. The combination of these statistics provides information for inferring the aggregational pattern of fish around and away from the shipwreck. This is the focus of discussion in this section.

Before dusk, PDF$_{AW1}$ always exhibited a significant non-Rayleigh shape with heavy tails [higher probability than Rayleigh at high echo magnitude region; indicated by the black arrow in Fig. 3(C), panel 1]. As fish started to emerge from the shipwreck, PDF$_{AW1}$ became increasingly heavier-tailed [Fig. 3(C), panels 1 to 3], which corroborates with the increase of $E_{max,AW1}$ and E_T at dusk [Fig. 3(B) upper panel and Fig. 4(B)]. Later in the night when more and more fish emerged and dispersed away from the shipwreck, PDF$_{AW1}$ trended back toward the Rayleigh distribution [Fig. 3(C), panel 4], but with a much higher mode (location of the peak of the echo pdf, indicated by the hollow arrow) compared to before dusk.

The shape of PDF$_{AW2}$ was very Rayleigh-like before dusk, representing the "noise-like" echoes from an empty water column [Fig. 3(C), panel 1]. As fish started to emerge from the shipwreck and disperse into AW2, PDF$_{AW2}$ deviated slightly from the Rayleigh distribution [Fig. 3(C), panel 2]. This is due to the fact that AW2 was only partially occupied by fish [Fig. 3(A), panel 2], leading to a mixture of stronger echoes from the fish and weaker echoes from the empty water column. Once AW2 became filled by the dispersed fish, PDF$_{AW2}$ trends toward the Rayleigh distribution [Fig. 3(C), panels 3 and 4] due to echoes from the numerous fish occupying the analysis window. Note the higher mode of the distribution here compared to when AW2 enclosed only a water column that was likely empty [Fig. 3(C), panel 1].

The above changes in the echo pdfs are also observed using the scintillation index SI [Fig. 3(B), bottom panel], which varies according to the degree to which a pdf deviates from the Rayleigh distribution ($SI = 1$). SI_{AW1} was much larger than 1 (highly non-Rayleigh) before dusk and during fish emergence, and slowly decreased toward 1 (more Rayleigh-like) until about 2230 when more and more fish dispersed to surround the shipwreck. This progression was reversed much more rapidly around dawn (~0500). In contrast, SI_{AW2} were mostly close to 1 (Rayleigh-like) except for during dusk and dawn, when the analysis window was only partially occupied by fish (~2000 and ~0500) and contained a mixture of echoes with different mean amplitudes.

One plausible interpretation of the observed statistics change in AW1 is the transition of dominant scattering sources from the shipwreck to fish from dusk to midnight. In this scenario, before dusk, the shipwreck itself dominated the scattering originating from the location of the shipwreck [Fig. 3(C), panel 1] and contributed principally to the heavy tail of PDF$_{AW1}$. The heavy tail with non-Rayleigh slope was the result of scattering from a finite number of highlights of the wreck in combination with the strong modulation of echo amplitudes due to highlight positions in the directional sonar beam (Chu and Stanton, 2010; Jones et al., 2017). The overall non-Rayleigh shape of the PDF$_{AW1}$ was due to the mixture of the strong shipwreck echo and the "noise-like" echoes from the empty water column enclosed in AW1. The latter component is indicated by the mode of the echo pdf (hollow arrow). At dusk, fish that hid inside the shipwreck during the day (and thus shielded from the sonar) started to
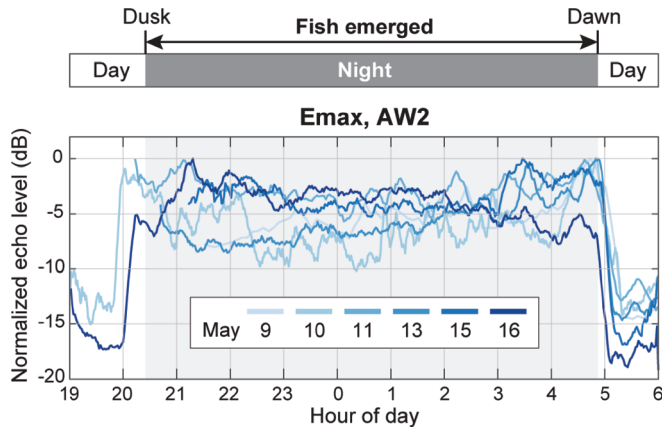
FIG. 5. (Color online) Comparison of the time series of $E_{max,\,AW2}$ across six overnight experimental sessions. To facilitate inter-session comparison, each time series was normalized by the maximum echo level during that night and smoothed using a running window across ten pings. See Table I for details of the selected waveforms. The times of dusk and dawn shown were averaged over the six nights.

emerge. Their additional scattering contribution led to the rapid increase of the tail of PDF_{AW1} and the level of $E_{max,\,AW1}$ and E_T. The high SI_{AW1} during this period may be explained by the intermittent masking of shipwreck highlights by dense clusters of the emerged fish in close proximity of the shipwreck. Toward midnight, the whole region was blanketed by fish as more continued to emerge from the shipwreck and dispersed away [Fig. 3(A), panel 4]. The ubiquitous presence of fish can cause significant masking of the shipwreck, while its large number led to the Rayleigh-like shape of PDF_{AW1} and the lower and more stable SI_{AW1} after 2230 [Fig. 3(C), panel 4]. In other words, fish scattering dominated AW1 during the night. $E_{max,\,AW1}$ slowly decreased during the course of the night, indicating the decreasing number of fish per unit area as a result of the night time dispersal of fish until the rapid convergence right before dawn.

An alternative scenario during daytime is that the shipwreck itself was never the dominant scatterer. Rather, the heavy tail and non-Rayleigh statistic could be from fish tightly congregating at the shipwreck location. In this scenario, the rapid increase of E_T at dusk may be explained by the release of heavy masking or extinction of sound through the dense fish congregation during daytime. The high scintillation before 2230 may be explained by the dense clusters of fish masking one another from the sonar.

Without ground truth observation on the fish's aggregation pattern and spatial relationship with respect to the shipwreck, the sonar echoes alone do not provide enough information to discriminate between the above two possible scenarios. In addition, we note that both $E_{max,\,AW1}$ and SI_{AW1} were high before dusk and after dawn, albeit not as high as during nighttime. The cause of these is unknown, as we do not have sufficient data during the day to explore these observations further.

V. FISH ECHO INFLUENCE ON SONAR PERFORMANCE

In this section, the influence of fish echo on sonar performance is discussed based on outputs of the split-window normalizer and characteristics of echo pdfs. The split-window normalizer is widely used to empirically detrend echo data and extract regions of interest in the absence of knowledge about absolute transmission loss and reverberation levels. The echo pdfs, obtained either empirically or theoretically, characterize the probability of an echo originating
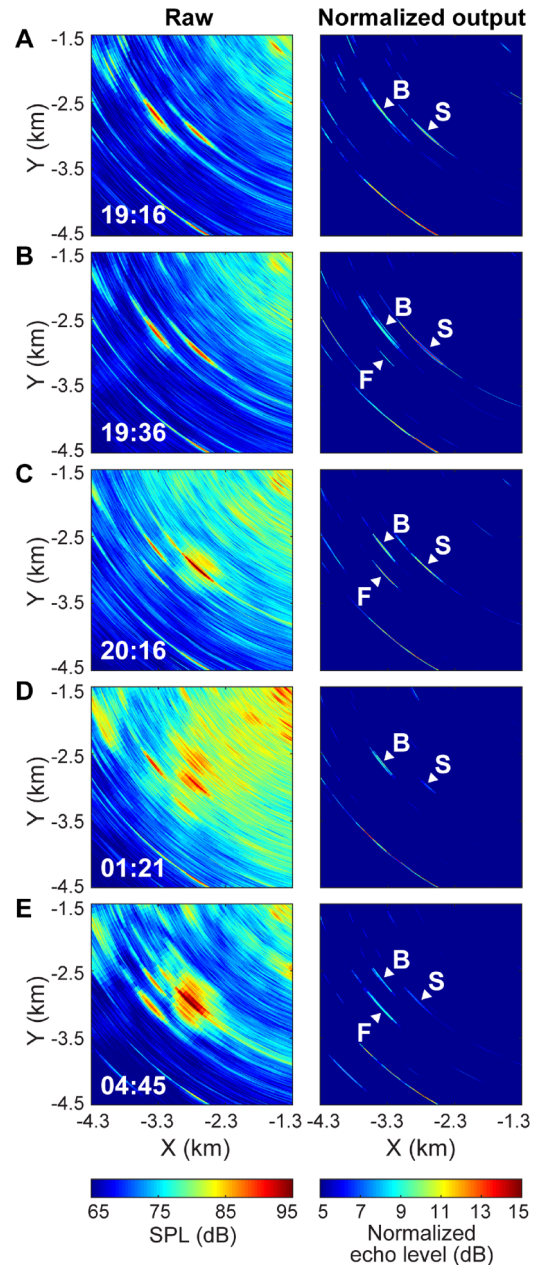

FIG. 6. (Color online) Influence of fish echoes on target detection. The normalized outputs (right column) were produced by the split-window normalizer, which performs detrending of raw echo returns (left column) in a data-driven manner. In (A) and (B), the normalizer accurately identifies the location of the shipwreck before large fish aggregations emerged from the wrecks. Compact fish aggregations were observed to produced target-like echoes in the normalizer output, as shown in (B), (C), and (E). Diffused fish aggregations produced reverberation-like echoes and partially obscured the prominent shipwreck echo in the normalizer output, as shown in (D) and (E). Note that in order to demonstrate the power of the split-window normalizer in detrending sonar returns, the raw echograms were not compensated by the $30 \log_{10} R$ range-varying gain, unlike in previous figures. B: Bridge span, S: USS Strength shipwreck, F: fish echo clutter.

J. Acoust. Soc. Am. **144** (3), September 2018

Lee *et al.*   1431

from target(s) of interest when an echo with a certain amplitude is received.

Outputs of the split-window normalizer show that echoes from a compact fish aggregation behave like those from targets and hinder detection of target of interest. Before fish emerged from the shipwreck, the split-window normalizer successfully pinpointed the locations of the shipwreck and the nearby bridge span [Figs. 6(A) and 6(B)]. This is expected, since these echo returns are distinctively stronger than the immediately adjacent background. However, analyses of $E_{max, AW1}$ and E_T have shown that it is highly possible that a large portion of echo energy observed at this location was from collocated dense fish aggregations (Secs. IV B and IV C). In other words, compact fish aggregations likely contributed significantly to these clutter-like echoes, which exhibited spatial extent and echo strength that are similar to those from targets of interest. A separate demonstration of fish echo clutter was found to the southwest of the shipwreck, where strong target-like echoes fluctuated in and out of the echogram over time [indicated by "F" in Figs. 6(B), 6(C), and 6(E)]. The transient nature of these echoes suggest that they were likely produced by fish that congregated to this location after nocturnal foraging.

At other times during the night, the fish dispersed to cover an extended spatial area and produced echoes that are stronger than those from the bottom. The signature of the strong echo originating from the shipwreck location was partially obscured by fish echoes in the normalizer output [Figs. 6(D) and 6(E)]. While the exact composition of echo sources at the shipwreck location during this time period is unknown, this observation demonstrates the potential of fish echoes in increasing reverberation level to reduce signal-to-noise ratio in target detection.

Echo statistics analysis yielded similarly intriguing results, showing that the variable forms of fish aggregation can substantially alter the overall characteristics of the echo pdf and affect the detection of targets of interest. Through the course of dusk fish emergence, the tail of PDF$_{AW1}$ became increasingly heavier, with the mode consistently moving toward higher echo amplitude [Fig. 3(C)]. These changes occurred while a relatively stable target-like signature was seen in the outputs of the split-window normalizer. After the majority of fish have emerged, the shape of the echo pdf trended back toward the Rayleigh distribution and therefore is more "noise-like," with a higher mean echo amplitude than the actual background. This Rayleigh-like shape of PDF$_{AW1}$ can be readily explained by the much more dispersed fish aggregation around the shipwreck, as opposed to the more compact aggregation before the emergence. The high variability of echo pdf features shown here indicates that an empirical echo pdf model from fish clutter should be considered time-dependent, and that physics-based models incorporating fish aggregation structure and behavior are needed to correctly and accurately interpret echoes from fish clutter (Gelb *et al.*, 2010; Jones *et al.*, 2014).

VI. DISCUSSION

In this study, strong diel reef fish movements over a horizontal scale of several kilometers were observed around a shallow-water artificial reef (shipwreck) in the northern Gulf of Mexico using a horizontal-looking mid-frequency sonar system. The fish behavior was in synchrony with the light cycle: they emerged rapidly from the artificial reef at dusk, dispersed into the surrounding area during the night, and converged back to the reef rapidly at dawn (Fig. 2, Mm. 1, Mm. 2). This observation corroborates with previous reports of the twilight foraging migration of many reef fish species (Appeldoorn *et al.*, 2009). In particular, the two most probable dominant fish species at our study site [Fig. 1(C); Sec. II C] are known to occur in enormous abundance at artificial reef sites, and both exhibit distinct nocturnal foraging behavior by dispersing from daytime shelter (Appeldoorn *et al.*, 2009; Arena *et al.*, 2007; Patterson *et al.*, 2013).

Our sonar study delivered a rare, macroscopic observation of reef fish behavior on the level of aggregations, and may have implications in ecological studies and resource management. Previous reef fish studies rely primarily on optics-based survey and tagging of individual fish (e.g., Appeldoorn *et al.*, 2009; Myers *et al.*, 2016; Nagelkerken *et al.*, 2000). The coverage and resolution of such data are inherently limited in both time and space due to the short observation range and labor-intensive nature of these sampling approaches. In sharp contrast, analyses of fish echoes from horizontal sonar observation could provide estimates such as the total biomass of fish residing in reefs and the proportion of fish engaged in foraging migration, in a much more synoptic manner. By utilizing different habitats for foraging and shelter, reef fish plays an important role in transferring energy across various environments in an ecosystem (Clark *et al.*, 2009). Information derived from horizontal sonar observations like ours can be crucial in evaluating the cost and benefit of artificial reef deployment, which has been controversial in achieving resource management goals through artificial manipulation of marine habitats (Bohnsack, 1989; Pickering and Whitmarsh, 1997).

From the perspective of sonar surveillance applications, our analyses show that the variable forms of fish echoes, though complex, have a clear time-dependence, and the knowledge of this time-dependence can be exploited and incorporated into an environmental awareness tool kit. We found that compact fish aggregations can elicit target-like echoes, and that spatially extended fish aggregations can produce increased reverberation level at night. In both cases, the characteristics of echoes can vary dramatically depending on the spatial structure of the aggregation. In addition, echoes from densely aggregated fish can greatly alter the apparent echo signature of the shipwreck, as demonstrated by the rapidly changing maximum echo level and echo pdf features over the course of the dusk emergence of foraging fish. These results collectively show the significant influence of fish scattering on the statistics widely used to characterize echoes from targets of interest. To distinguish fish from typical targets, further field work is desired where wider bandwidth signals are used to investigate resonance phenomenon often associated with scattering from fish with swimbladders.

While observations of fish using horizontal-looking sonars have been reported since the 1960s, the combination

of the experimental setup and environment in TREX13 granted a unique opportunity to investigate long-range fish echoes and their impacts on sonar performance. The relatively simple propagation environment created by a shallow and well-mixed water column, in combination with the fixed source and receiver pair and the moderate signal bandwidth, significantly reduced the ambiguity in our interpretation. Specifically, potential confounding factors such as the presence of convergence or shadow zones and uncertainties associated with variable source or receive locations were mitigated. The highly predictable timing and movement pattern of the reef fish revealed in our study suggests that the artificial reef environment is an outstanding natural experimental ground for future study of fish echo influence on sonar performance.

To achieve better capability in modeling, predicting, and interpreting fish echoes for both ecological studies and sonar surveillance applications, additional biological ground truth is needed. Of particular importance are (1) the species composition and size distribution of fish at the artificial reef site, and (2) the vertical distribution of fish across day and night. These data can be obtained by optics- or net-based methods (for obtaining fish composition) and vertical-looking echosounder observations (for resolving depth variation of fish). The above biological parameters will help determine the approximate size of the fish swimbladder, which is intimately related to its resonance frequency and scattering strength. Such information is crucial in developing predictive, physics-based models for both the absolute scattering level and statistical characteristics of fish echoes, and will allow detailed investigation into the potential occurrence of multiple scattering or acoustic shadowing in natural environments.

Building on previous studies of long-range fish echoes, our study further substantiates the utility of horizontal-looking sonar systems as an ecosystem monitoring tool by demonstrating its macroscopic observational capability. Along with the recent increase of strategic importance of shallow water environments where numerous fish populates, our results underscore the importance of considering the influence of fish echoes on sonar performance.

ACKNOWLEDGMENTS

Abraham, D. A., and Willett, P. K. (**2002**). "Active sonar detection in shallow water using the page test," IEEE J. Ocean. Eng. **27**, 35–46.

Appeldoorn, R. S., Aguilar-Perera, A., Bouwmeester, B. L. K., Dennis, G. D., Hill, R. L., Merten, W., Recksiek, C. W., and Williams, S. J. (**2009**). "Movement of fishes (Grunts: Haemulidae) across the coral reef seascape: A review of scales, patterns and processes," Caribb. J. Sci. **45**, 304–316.

Arena, P. T., Jordan, L. K. B., and Spieler, R. E. (**2007**). "Fish assemblages on sunken vessels and natural reefs in southeast Florida, USA," Hydrobiologia **580**, 157–171.

Benoit-Bird, K. J., and Lawson, G. L. (**2016**). "Ecological insights from pelagic habitats acquired using active acoustic techniques," Ann. Rev. Mar. Sci **8**, 463–490.

Bohnsack, J. A. (**1989**). "Are high densities of fishes at artificial reefs the results of habitat limitation or behavioural preference?," Bull. Mar. Sci. **44**, 631–645.

Botev, Z. I., Grotowski, J. F., and Kroese, D. P. (**2010**). "Kernel density estimation via diffusion," Ann. Stat. **38**, 2916–2957.

Chu, D., and Stanton, T. K. (**2010**). "Statistics of echoes from a directional sonar beam insonifying finite numbers of single scatterers and patches of scatterers," IEEE J. Ocean. Eng. **35**, 267–277.

Clark, R. D., Pittman, S., Caldow, C., Christensen, J., Roque, B., Appeldoorn, R. S., and Monaco, M. E. (**2009**). "Nocturnal fish movement and trophic flow across habitat boundaries in a coral reef ecosystem (SW Puerto Rico)," Caribb. J. Sci. **45**, 282–303.

Farmer, D. M., Trevorrow, M. V., and Pedersen, B. (**1999**). "Intermediate range fish detection with a 12-kHz sidescan sonar," J. Acoust. Soc. Am. **106**, 2481–2490.

Fialkowski, J. M., and Gauss, R. C. (**2010**). "Methods for identifying and controlling sonar clutter," IEEE J. Ocean. Eng. **35**, 330–354.

Fulton, C. J., Bellwood, D. R., and Wainwright, P. C. (**2005**). "Wave energy and swimming performance shape coral reef fish assemblages," Proc. Biol. Sci. **272**, 827–832.

Gallaudet, T. C., and de Moustier, C. P. (**2003**). "High-frequency volume and boundary acoustic backscatter fluctuations in shallow water," J. Acoust. Soc. Am. **114**, 707–725.

Gauss, R. C., Fialkowski, J. M., Kunz, E. L., Menis, R., Stanton, T. K., Sellers, C. J., and Jech, J. M. (**2009**). "Clutter variability due to fish aggregations: Mid-frequency measurements in the Gulf of Maine," in *Proceedings of the 3rd International Conference and Exhibition on Underwater Acoustic Measurements: Technologies & Results*, June 21–26, Nafplion, Greece, pp. 459–466.

Gauss, R., Fromm, D., LePage, K., Fialkowski, J., and Nero, R. (**2004**). "The influence of the sea surface and fish on long-range reverberation," in *High Frequency Ocean Acoustics: High Frequency Ocean Acoustics Conference (AIP Conference Proceedings)*, March 1–5, La Jolla, CA, pp. 157–164.

Gelb, J. M., Heath, R. E., and Tipple, G. L. (**2010**). "Statistics of distinct clutter classes in midfrequency active sonar," IEEE J. Ocean. Eng. **35**, 220–229.

Haralabus, G., and Baldacci, A. (**2006**). "Unambiguous triplet array beamforming and calibration algorithms to facilitate an environmentally adaptive active sonar concept," in *Proceedings of Oceans 2006*, September 18–22, Boston, MA.

Hefner, B. T., and Tang, D. (**2017a**). "Guest Editorial Target and Reverberation Experiment 2013 (TREX13)—Part I," IEEE J. Ocean. Eng. **42**, 247–249.

Hefner, B. T., and Tang, D. (**2017b**). "Guest Editorial Target and Reverberation Experiment 2013 (TREX13)—Part II," IEEE J. Ocean. Eng. **42**, 757–758.

Jones, B. A., Colosi, J. A., and Stanton, T. K. (**2014**). "Echo statistics of individual and aggregations of scatterers in the water column of a random, oceanic waveguide," J. Acoust. Soc. Am. **136**, 90–108.

Jones, B. A., Stanton, T. K., Colosi, J. A., Gauss, R. C., Fialkowski, J. M., and Michael Jech, J. (**2017**). "Broadband classification and statistics of echoes from aggregations of fish measured by long-range, mid-frequency sonar," J. Acoust. Soc. Am. **141**, 4354–4371.

Lee, W.-J., and Stanton, T. K. (**2014**). "Statistics of echoes from mixed assemblages of scatterers with different scattering amplitudes and numerical densities," IEEE J. Ocean. Eng. **39**, 740–754.

Lee, W.-J., and Stanton, T. K. (**2016**). "Statistics of broadband echoes: Application to acoustic estimates of numerical density of fish," IEEE J. Ocean. Eng. **41**, 709–723.

Makris, N. C., Ratilal, P., Jagannathan, S., Gong, Z., Andrews, M., Bertsatos, I., Godø, O. R., Nero, R. W., and Jech, J. M. (**2009**). "Critical population density triggers rapid formation of vast oceanic fish shoals," Science **323**, 1734–1737.

Makris, N. C., Ratilal, P., Symonds, D. T., Jagannathan, S., Lee, S., and Nero, R. W. (**2006**). "Fish population and behavior revealed by instantaneous continental shelf-scale imaging," Science **311**, 660–663.

Medwin, H., and Clay, C. S. (**1998**). *Fundamentals of Acoustical Oceanography* (Academic Press, San Diego, CA).

Myers, E. M. V., Harvey, E. S., Saunders, B. J., and Travers, M. J. (**2016**). "Fine-scale patterns in the day, night and crepuscular composition of a temperate reef fish assemblage," Mar. Ecol. **37**, 668–678.

Nagelkerken, I., Dorenbosch, M., Verberk, W. C. E. P., Cocheret De La Morinière, E., and Van Der Velde, G. (**2000**). "Day-night shifts of fishes between shallow-water biotopes of a Caribbean bay, with emphasis on the nocturnal feeding of Haemulidae and Lutjanidae," Mar. Ecol. Prog. Ser. **194**, 55–64.

Nieto, E. (**2013**). "USS Strength Wreck Dive," https://www.youtube.com/watch?v=PZmxMFL5osw (Last viewed June 19, 2017).

Orange, D. L., and Garcia-Garcia, A. (**2010**). "Integration of all data collected to evaluate seasonal variability in seafloor and shallow sub-surface acoustic properties, shallow water Gulf of Mexico," ONR Annual Report No. N00014-10-1-0583, ONR, Arlington, VA.

Patterson, W. F., Tarnecki, J. H., Addis, D. T., and Barbieri, L. R. (**2013**). "Reef fish community structure at natural versus artificial reefs in the northern Gulf of Mexico," in *Proceedings of the 66th Annual Meeting of the Gulf and Caribbean Fisheries Institute*, November 4–8, Corpus Christi, TX.

Pedersen, B., and Trevorrow, M. V (**1999**). "Continuous monitoring of fish in a shallow channel using a fixed horizontal sonar," J. Acoust. Soc. Am. **105**, 3126–3135.

Pickering, H., and Whitmarsh, D. (**1997**). "Artificial reefs and fisheries exploitation: A review of the 'attraction versus production' debate, the influence of design and its significance for policy," Fish. Res. **31**, 39–59.

Rusby, J. S. M., Somers, M. L., Revie, J., McCartney, B. S., and Stubbs, A. R. (**1973**). "An experimental survey of a herring fishery by long-range sonar," Mar. Biol. **22**, 271–292.

Stanton, T. K. (**1985**). "Volume scattering: Echo peak PDF," J. Acoust. Soc. Am. **77**, 1358–1366.

Stanton, T. K. (**2012**). "30 years of advances in active bioacoustics: A personal perspective," Methods Oceanogr. **1–2**, 49–77.

Stanton, T. K., Chu, D., Gelb, J. M., Tipple, G. L., and Baik, K. (**2015**). "Interpreting echo statistics of three distinct clutter classes measured with a midfrequency active sonar: Accounting for number of scatterers, scattering statistics, and beampattern effects," IEEE J. Ocean. Eng. **40**, 657–665.

Stanton, T. K., Lee, W.-J., and Baik, K. (**2018**). "Echo statistics associated with discrete scatterers: A tutorial on physics-based methods" (in press).

Stanton, T. K., Sellers, C. J., and Jech, J. M. (**2012**). "Resonance classification of mixed assemblages of fish with swimbladders using a modified commercial broadband acoustic echosounder at 1–6 kHz," Can. J. Fish. Aquat. Sci. **69**, 854–868.

Stolk, P., Markwell, K., and Jenkins, J. M. (**2007**). "Artificial reefs as recreational scuba diving resources: A critical review of research," J. Sustain. Tour. **15**, 331–350.

Tollefsen, C., and Pecknold, S. (**2014**). "Using physical oceanography to improve transmission loss calculations in undersampled environments," J. Acoust. Soc. Am. **136**, 2298–2298.

Urick, R. J. (**1983**). *Principles of Underwater Sound* (McGraw-Hill, New York).

Weston, D. E., and Andrews, H. W. (**1990**). "Seasonal sonar observations of the diurnal shoaling times of fish," J. Acoust. Soc. Am. **87**, 673–680.

Weston, D. E., and Revie, J. (**1971**). "Fish echoes on a long-range sonar display," J. Sound Vib. **17**, 105–112.

Yang, J., Tang, D., Hefner, B. T., Williams, K. L., and Preston, J. R. (**2018**). "Overview of mid-frequency reverberation data acquired during the Target and Reverberation Experiment 2013," IEEE J. Ocean. Eng. **43**, 563–585.